Ocean Engineering 129 (2017) 291–300

Contents lists available at ScienceDirect

Ocean Engineering

journal homepage: www.elsevier.com/locate/oceaneng

Transient analysis of micro-hydrokinetic turbines for river applications

C. Daskiran[a,b], J. Riglin[a], W. Schleicher[a], A. Oztekin[a,*]

[a] Mechanical Engineering and Mechanics, P. C. Rossin School of Engineering and Applied Science, Lehigh University, Bethlehem, PA 18015, USA
[b] Turkish Military Academy, Department of Mechanical Engineering, Ankara, Turkey

ARTICLE INFO

Keywords:
Micro-hydrokinetic
River applications
Turbulence
CFD
Transient analysis

ABSTRACT

Transient simulations are conducted to characterize a single turbine and multiple turbines in an inline and a staggered array using k-ω shear-stress transport (SST) turbulence model. Performance characteristics predicted by transient analysis at various operating conditions were compared to those predicted by steady-state analysis. Transient results indicated that a power coefficient of 0.43 would be generated at the best efficiency point which corresponds to 1.4% deviations between transient and steady-state solutions for a single unit. Flow separation is observed at the tip speed ratio lower than that at the design point. The relative power of the upstream turbine is obtained to be nearly unity in both inline and staggered arrays. The relative power of the downstream turbine in the staggered array is not influenced by the presence of the upstream turbine and it is the same as that of the upstream turbine. On the other hand, the relative power of the downstream turbine in an inline array is reduced to 0.18 at a downstream separation of $6D_t$. The massive drop in the power generation by the downstream turbine resulted from the presence of strong wake flow induced by the upstream turbine.

1. Introduction

Conventional hydropower generation in the United States represents nearly half of the nation's annual renewable energy capacity (Conti et al., 2015). Traditional hydro projects require large capital investments, civil structures, and may result in a negative impact among local aquatic life. Much of the remaining hydropower resource potential exists in the form of rivers and tides. This largely untapped power source may be exploited using marine and hydrokinetic (MHK) technology. It is estimated that approximately 1,381 TWh/yr of power could be generated in the United States by employing MHK technologies. Conservative estimates from the same study predict 120 TWh/yr of the total power is technically recoverable (Ravens et al., 2012).

The micro-hydro regime is generally considered to be between 0.5 and 100 kW of power, approximately the minimum demand for a small family or business (Jenkins, 2013). Despite reduced power production, the small systems generally offer portability. These characteristics are especially desirable in temporary encampment situations such as military field operations and humanitarian operations in rural areas. A photovoltaic battery system called the Ground Renewable Expeditionary Energy System, or GREENS, has been developed for use by the U.S. Marine Corps to produce 300 W of continuous power to run these encampments (U.S. Marine Corps, 2012). A secondary source of power is necessary when sunlight is not available. Therefore, designing an array of micro-hydrokinetic turbines that could meet the power requirements and interface with the system would be advantageous.

Multiple configurations of hydrokinetic turbine designs have been investigated. Most studies, however, have been focused on horizontal axis turbines. The primary benefit of vertical axis turbines is that it is operable under any flow direction with the tradeoff being lower attainable efficiencies. For river applications, it is generally more economical to use horizontal axis turbines due to the improved efficiency considering localized potential power limitations and knowledge of expected flow direction. Batten et al. (2006, 2007, 2008) used a blade element methodology (BEM) to design horizontal axis hydrokinetic turbines for tidal applications. They validated BEM simulations by testing a scaled model in a cavitation tunnel. Mukherji et al. (2011) compared BEM with CFD for a horizontal axis hydrokinetic turbine, and investigated the effect of solidity, angle of attack, and number of blades on power generation. Experimental studies by Myers and Bahaj (2006) and Bahaj et al. (2007) demonstrated that the blade twist distribution and rotor yaw angle affect the lift and the drag and the mechanical power output.

Hwang et al. (2009) studied a vertical axis turbine that actively controlled blade attack to maximize power output and improved self-start. A 25% improvement in performance compared to pure cycloidal motion for the same operating conditions was observed through controlling the angle of attack of each individual blade based on the oncoming flow. Hayati et al. (2012) investigated the effect of rake angle

* Corresponding author.
E-mail address: alo2@lehigh.edu (A. Oztekin).

http://dx.doi.org/10.1016/j.oceaneng.2016.11.020
Received 27 February 2016; Received in revised form 30 August 2016; Accepted 17 November 2016
0029-8018/

Nomenclature

Full Scripts

b	designated domain side
C	coefficient
c	chord length, m
D	diameter, m
e	error, %
F	blending function
GCI	grid convergence index, %
k	turbulent kinetic energy, J/kg
L	length scale, m
m	meridional length, m
N	number of cells
p	pressure, Pa
$\tilde{p}$	normalized pressure
P	power, W
$\tilde{P}$	relative power
r	refinement factor
R	radius of rotor tip, m
S	mean rate-of-strain tensor, 1/s
s	blade spacing, m
t	time, s
t	thickness, m
T	thrust, N
λ	tip speed ratio
U	velocity, m/s
$\tilde{U}$	normalized velocity
Z	quantity

Greek Symbols

α, β, σ	closure coefficients.
β	relative angle, °.
Δ	change in variable.
ε	permutation symbol.
θ	wrap angle, °.
μ	dynamic viscosity, Pa-s.
ν	kinematic viscosity, m^2/s.
ξ	local tip-speed ratio.
ρ	density, kg/m^3.
σ	solidity.
φ	dummy variable.
ψ	stagger angle, °.
ω	angular velocity, 1/s.
ω	specific dissipation rate, 1/s.
$\tilde{\omega}$	normalized vorticity.

Superscript

*	denotes a closure coefficient.
‘	denotes the blade angle.

Subscripts

a	absolute.
A	single unit performance.
B	blades.
ext	extrapolated.
H	hydraulic.
h	at the hub.
$k, \omega, \omega2$	denotes different colure coefficients.
i,j,k,l,s,t	tensor indices.
I	input.
m	at the mean value.
O	output.
r	relative.
T	turbulent / thrust.
t	at the tip.

on marine propeller performance and concluded that observed thrust performance improves as the rake angle is increased for conventional propeller design. Modifying rake angles may allow for improvements to be made in propeller operation where energy absorption is the primary design goal instead of thrust generation.

Schleicher et al. (2013, 2014a, 2014b, 2015) and Riglin et al., (2013, 2014, 2015a, 2015b) have conducted numerous analyses on compact turbine designs and configurations to produce 0.5 kW. In Schleicher et al. (2015), a portable MHK turbine was designed using a bottom up approach with the overall blade design as small as possible in order to adhere to power, weight, size requirements and limitations. Riglin et al. (2015a) characterized turbine performance when multiple diffuser designs were introduced. Experimental analyses were conducted on shroud and diffuser designs for marine current turbine applications by Shahsavarifard et al. (2015). Turbine performance was predicted with steady-state simulations using OpenFOAM (ESI-OpenCFD, 2014) and the peak efficiency of 0.43 nearly matched the specified initial design condition. Schleicher et al. (2015) expanded on that work to further optimize the preliminary design to encompass a greater operating range in terms of both flow speed and deployment (Schleicher et al., 2013, 2014a, 2014b, 2014c). The rotor design was modeled with multiple phases by Riglin et al. (2015b) to more accurately capture the effects of operation near the free surface, resulting in expected mechanical losses of 33%. Riglin et al. (2015b) and Noruzi et al. (2015) both analyze turbine performance near the free surface, with the goal of determining suitable installation depths to

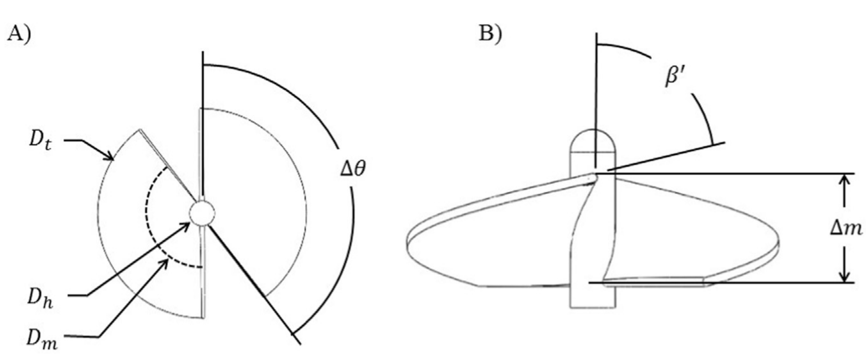

Fig. 1. Blade geometry design A) front view and B) top view.